THE JOURNAL OF BIOLOGICAL CHEMISTRY
Vol. 279, No. 4, Issue of January 23, pp. 2975–2983, 2004

Printed in U.S.A.

Glycosylation Is Important for Cell Surface Expression of the Water Channel Aquaporin-2 but Is Not Essential for Tetramerization in the Endoplasmic Reticulum*

Received for publication, September 30, 2003, and in revised form, October 30, 2003
Published, JBC Papers in Press, October 30, 2003, DOI 10.1074/jbc.M310767200

Giel Hendriks, Marco Koudijs, Bas W. M. van Balkom‡, Viola Oorschot, Judith Klumperman, Peter M. T. Deen‡, and Peter van der Sluijs§

From the Department of Cell Biology, University Medical Center Utrecht, Utrecht 3584 CX and the ‡Department of Physiology, University Medical Center, Nijmegen 6500 HB, The Netherlands

Aquaporin-2 (AQP2) is a pore-forming protein that is required for regulated reabsorption of water from urine. Mutations in AQP2 lead to nephrogenic diabetes insipidus, a disorder in which functional AQP2 is not expressed on the apical cell surface of kidney collecting duct principal cells. The mechanisms and pathways directing AQP2 from the endoplasmic reticulum to the Golgi complex and beyond have not been defined. We found that ~25% of newly synthesized AQP2 is glycosylated. Nonglycosylated and complex-glycosylated wild-type AQP2 are stable proteins with a half-life of 6–12 h and are both detectable on the cell surface. We show that AQP2 forms tetramers in the endoplasmic reticulum during or very early after synthesis and reaches the Golgi complex in 1–1.5 h. We also report that glycosylation is neither essential for tetramerization nor for transport from the endoplasmic reticulum to the Golgi complex. Instead, the *N*-linked glycan is important for exit from the Golgi complex and sorting of AQP2 to the plasma membrane. These results are important for understanding the molecular mechanisms responsible for the intracellular retention of AQP2 in nephrogenic diabetes insipidus.

Aquaporins (AQPs)[1] are ubiquitously expressed pore-forming proteins that facilitate water transport across membranes along an osmotic gradient (see Ref. 1). AQPs share a highly conserved domain organization with six transmembrane domains and cytoplasmically oriented N and C termini. AQPs form tetramers or sometimes higher order oligomers in membranes. Structural studies of AQP1 revealed that the functional unit is a tetramer with each monomer providing an independent water pore (2). Stability of the tetramer is thought to be conferred by the assembly of monomers as a tight fitting wedge within the tetramer.

With the exception of AQP2, which is regulated by the antidiuretic hormone vasopressin, most of the AQPs are expressed constitutively at the plasma membrane (see Ref. 3). AQP2 is localized in a tubulovesicular subapical storage compartment. The intracellular retention is thought to be caused by tethering of the storage vesicles to the actin cytoskeleton and is regulated by members of the rho subfamily of small GTPases (4). Binding of vasopressin to the basolateral V2 receptor increases cAMP concentration which activates protein kinase A. Protein kinase A phosphorylates AQP2-Ser^{256} which is required for fusion of AQP2 storage vesicles with the plasma membrane (5, 6). The precise mechanism responsible for the recruitment of tetrameric AQP2 to the cell surface is not known, but phosphorylation of at least three of the four monomers, reportedly, is required and sufficient for the localization of AQP2 on the plasma membrane (7). The regulated recruitment of plasma membrane proteins from intracellular storage vesicles provides an efficient means to control cell surface expression and was originally discovered for the insulin-regulated glucose transporter GLUT4 (see Ref. 8). GLUT4 and AQP2 translocation share some similarities such as the requirement for the v-SNARE synaptobrevin-2 in fusion with the plasma membrane (8, 9). Nevertheless, there are important differences. For instance, GLUT4 translocates from a basolateral storage compartment in polarized epithelial cells, and phosphorylation of GLUT4 inhibits glucose transport, whereas phosphorylation of AQP2 is essential for its recruitment from an apical storage compartment.

Despite the progress that has been made in understanding the physiology of AQP-mediated water transport, important aspects such as biosynthetic maturation and intracellular transport of AQP water channels are incompletely understood. For instance, it has been shown for AQP1 that conformational changes and rearrangements take place during insertion in the endoplasmic reticulum (ER), but whether insertion occurs co-translationally or post-translationally has become a controversial issue (10, 11). In addition, with the exception of AQP4 (12), the sorting signals required for transport of AQPs between intracellular compartments remain to be defined. The observations that AQP2 and AQP6 (13) reside in distinct intracellular compartments and the other AQPs localize to the plasma membrane suggest that crucial differences exist in sorting mechanisms of the AQPs.

The consensus *N*-linked glycosylation site in AQP1 and AQP2 is used inefficiently. Most of the AQP1 and AQP2 molecules on the cell surface remain unglycosylated (14, 15). Intriguingly, AQP2-T125M, a mutant that causes recessive nephrogenic diabetes insipidus (NDI) (16, 17), is not glycosylated because the consensus *N*-linked glycosylation motif is dis-

* This work was supported by The Netherlands Organization for Medical Research (to P. v. d. S. and P. M. T. D.). The costs of publication of this article were defrayed in part by the payment of page charges. This article must therefore be hereby marked "*advertisement*" in accordance with 18 U.S.C. Section 1734 solely to indicate this fact.

§ To whom correspondence should be addressed: Dept. of Cell Biology, University Medical Center Utrecht, AZU Rm. G02.525, Heidelberglaan 100, Utrecht 3584 CX, The Netherlands. Tel.: 31-30-250-7574; Fax: 31-30-254-1797; E-mail: pvander@knoware.nl

[1] The abbreviations used are: AQP(s), aquaporin(s); BFA, brefeldin A; CHO cells, Chinese hamster ovary cells; EGFP, enhanced green fluorescent protein; Endo H, endoglycosidase H; ER, endoplasmic reticulum; GFP, green fluorescent protein; MDCK cells, Madin-Darby canine kidney cells; NDI, nephrogenic diabetes insipidus; PNGase F, peptide *N*-glycosidase F; SNARE, soluble NSF attachment protein receptors; TGN, *trans*-Golgi network; PDI, protein disulfide isomerase.

rupted. This mutant is absent from the plasma membrane (17), suggesting that it is misfolded and retained in the ER, or for some other reason does not reach the cell surface. The significance of this observation transcends well beyond the particular AQP2-T125M patient mutant because it translates directly into two general questions relating to mechanisms responsible for ER quality control of AQPs and how nonglycosylated wild-type AQP2 is normally targeted to the plasma membrane.

Mutations in AQP2 result in NDI (see Ref. 18) through two putative mechanisms. Recessive nonfunctional mutants are thought to be retained in the ER and fail to tetramerize, whereas dominant AQP2 mutants oligomerize with the product of the wild-type allele, forming tetramers that are improperly targeted and do not reach the apical cell surface (19, 20). Given the consequences of mutant AQP2 alleles for the health of affected individuals, surprisingly little is known about biosynthetic maturation and sorting of AQP2. To develop rationally therapeutic protocols for NDI, we need to understand the pathways of wild-type AQP2 to the cell surface. Earlier studies with tunicamycin were interpreted to indicate that glycosylation was not essential for AQP2 shuttling (15). Given the recent findings that this glycosylation inhibitor severely affects multiple ER and secretory pathway functions (21, 22), a reevaluation of the significance of glycosylation in AQP2 function became necessary. Using biochemical and morphological methods, we show that tetramerization of AQP2 occurs in the ER and that *N*-linked glycosylation is important for its transport from the Golgi complex to post-Golgi compartments.

EXPERIMENTAL PROCEDURES

Reagents—AQP2-N123Q was constructed by overlap extension PCR and ligated in pcDNA3 (Invitrogen). Synthetic cDNAs were verified by restriction analysis and dye termination sequencing. Furin-pEGFP was generously provided by Gary Thomas. Antibodies against the C terminus of AQP2 were raised in rabbits and guinea pigs as described (23). The following antibodies were used: rabbit anti-protein disulfide isomerase and rabbit anti-calnexin (Ineke Braakman, University of Utrecht), mouse anti-gp114 (Kai Simons, Max Planck Institute, Dresden), mouse anti-CTR433 (Michel Bornens, Curie Institute, Paris), and mouse anti-α-tubulin Thomas Kreis, University of Geneva). The mouse antibodies against γ-adaptin and GM130 were from Transduction Labs, and conjugated secondary antibodies were purchased from Jackson Immunoresearch Laboratories and Molecular Probes.

Cell Culture and Transfection—Madin-Darby canine kidney type I (MDCK-I) cells expressing human wild-type AQP2, or vesicular stomatitis virus G-tagged AQP2-R187C were maintained as described (24). MDCK-I cells were transfected with AQP2-N123QpcDNA3 using the calcium phosphate method. CHO and CHO-15B cells were transfected with wild-type AQP2pcDNA3 and AQP2-N123QpcDNA3 in the same way. Stable transfectants were selected in medium containing 0.6 mg/ml G418 and screened by immunofluorescence microscopy and Western blot. Expression of cytomegalovirus-driven constructs was induced by culturing the cells for 14–17 h in the presence of 5 mM sodium butyrate.

Pulse-Chase and Immunoprecipitation—Cells were grown in 6-cm tissue culture dishes, washed with phosphate-buffered saline, and incubated for 30 min with methionine- and cysteine-free minimum Eagle's medium (Sigma). The cells were labeled for 30 min at 37 °C with 0.2 mCi/ml [^{35}S]methionine/cysteine (Redivue Promix, Amersham Biosciences) and chased for different periods of time in Dulbecco's modified Eagle's medium, 10% fetal calf serum, 1 mM methionine, 1 mM cysteine. Cells were lysed in 1 ml of 1% Triton X-100, 50 mM Tris, pH 7.4, 1 mM EDTA, and a protease inhibitor mix (Complete mini, Roche Applied Science) on ice. Detergent lysates were centrifuged at 14,000 rpm for 5 min to remove insoluble debris. Lysates were next precleared by incubation with bovine serum albumin-coated protein A beads for 1 h at 4 °C. The supernatants were then transferred to a fresh tube and incubated with antibody-coated beads for 2 h at 4 °C. Beads were washed three times at room temperature for 5 min with 0.05% Triton X-100, 0.1% SDS, 0.3 M NaCl, 10 mM Tris-HCl, pH 8.6. Endoglycosidase H (Endo H) and peptide *N*-glycosidase F (PNGase F) digestions were performed on immune precipitates as described previously (25). Samples were resuspended in 25 μl of Laemmli sample buffer containing 50 mM dithiothreitol, incubated for 30 min at 37 °C, and resolved by SDS-PAGE on 12.5% gels. Quantitation of immunoprecipitated AQP2 was done by phosphorimaging.

Immunoelectron Microscopy—MDCK-AQP2 and MDCK-AQP2-N123Q cells were fixed for immunoelectron microscopy with a mixture of 2% freshly prepared formaldehyde and 0.2% glutaraldehyde in 0.1 M phosphate buffer, pH 7.4. After 6 h at room temperature the fixative was replaced, and cells were postfixed in 2% formaldehyde overnight at 4 °C. Cells were then prepared for ultrathin cryosectioning and immunogold labeled according to the protein A-gold method. Briefly, fixed cells were washed once in phosphate-buffered saline with 0.02 M glycine, after which cells were scraped in 1% gelatin in phosphate-buffered saline and embedded in a 12% gelatin solution. The cell-gelatin mixture was solidified on ice and cut into small blocks. After infiltration with 2.3 M sucrose at 4 °C, blocks were mounted on aluminum pins and frozen in liquid nitrogen. Ultrathin cryosections were picked up in a mixture of 50% sucrose and 50% methyl cellulose (26) and incubated with a rabbit antibody against AQP2, which was used previously for the ultrastructural localization of AQP2 in *Xenopus* oocytes (27). Labeling was done with protein A coated with 10 nm of gold.

Miscellaneous Methods—Methods for cRNA injection in *Xenopus* oocytes, water permeability measurements, immunofluorescence microscopy, cell surface biotinylation, and velocity gradient centrifugation have been described previously (17, 19, 28). Confocal laser scanning immunofluorescence microscopy of MDCK cells was done as described previously (29).

RESULTS

Biosynthesis and Maturation of AQP2—To investigate the biosynthesis of AQP2 we used the MDCK cell line. These cells lack measurable levels of endogenous AQP2, whereas transfected AQP2 is subject to vasopressin-dependent translocation like AQP2 in the kidney (24). MDCK-AQP2 cells were pulse labeled with [^{35}S]methionine/cysteine, and AQP2 was immunoprecipitated from detergent lysates after different periods of chase time and analyzed by SDS-PAGE on 12.5% reducing gels. As shown in Fig. 1*A*, two bands of 29 and 31–32 kDa (which we refer to as 31 kDa) can be discerned which are not present in immunoprecipitates prepared from nontransfected cells (not shown). Quantification of the 29- and 31-kDa bands at the end of the 30-min pulse by phosphorimaging showed that they are formed at a ratio of 3:1. Even after a short pulse of 2.5 min, about 25% of newly synthesized AQP2 was present in the 31-kDa band, suggesting that glycosylation occurs cotranslationally or very shortly after translation. Whereas the 29-kDa form remained present at all chase times, the 31-kDa form disappeared within 1–1.5 h of chase, and at the same time, a complex of proteins appeared as a faint smear of 40–46 kDa. We then explored the relationship between the 29-, 31-, and the 40–46-kDa bands using Endo H and PNGase F digestions of AQP2 immunoprecipitates. As shown in Fig. 1*A*, Endo H selectively removed the 31-kDa band but not the 29-kDa and 40–46-kDa bands, whereas after PNGase F only the 29-kDa protein remained detectable as a doublet. PNGase F treatment causes oxidation of the asparagine to an aspartate in the consensus *N*-linked glycosylation sequence. This modification adds extra negative charge to the protein which might be responsible for a small shift in mobility on SDS-polyacrylamide gels. Alternatively, the hydrophobic transmembrane domains of AQP2, which represent ~50% of its mass, might fail to be completely denatured in SDS. This could limit the accessibility of the *N*-linked glycosylation site to PNGase F, preventing quantitative deglycosylation.

Disappearance of the 31-kDa band within 1 h after translation and the appearance of the 40–46-kDa bands indicate transport from the ER to the Golgi complex. Although some of 40–46-kDa material is already present at the end of the pulse period, it is unlikely that complex glycosylation of AQP2 occurs cotranslationally. Assuming a translation rate of 5–10 amino acids/s (25, 30), the pulse period is relatively long compared with the time it takes to translate the 270-amino acid protein

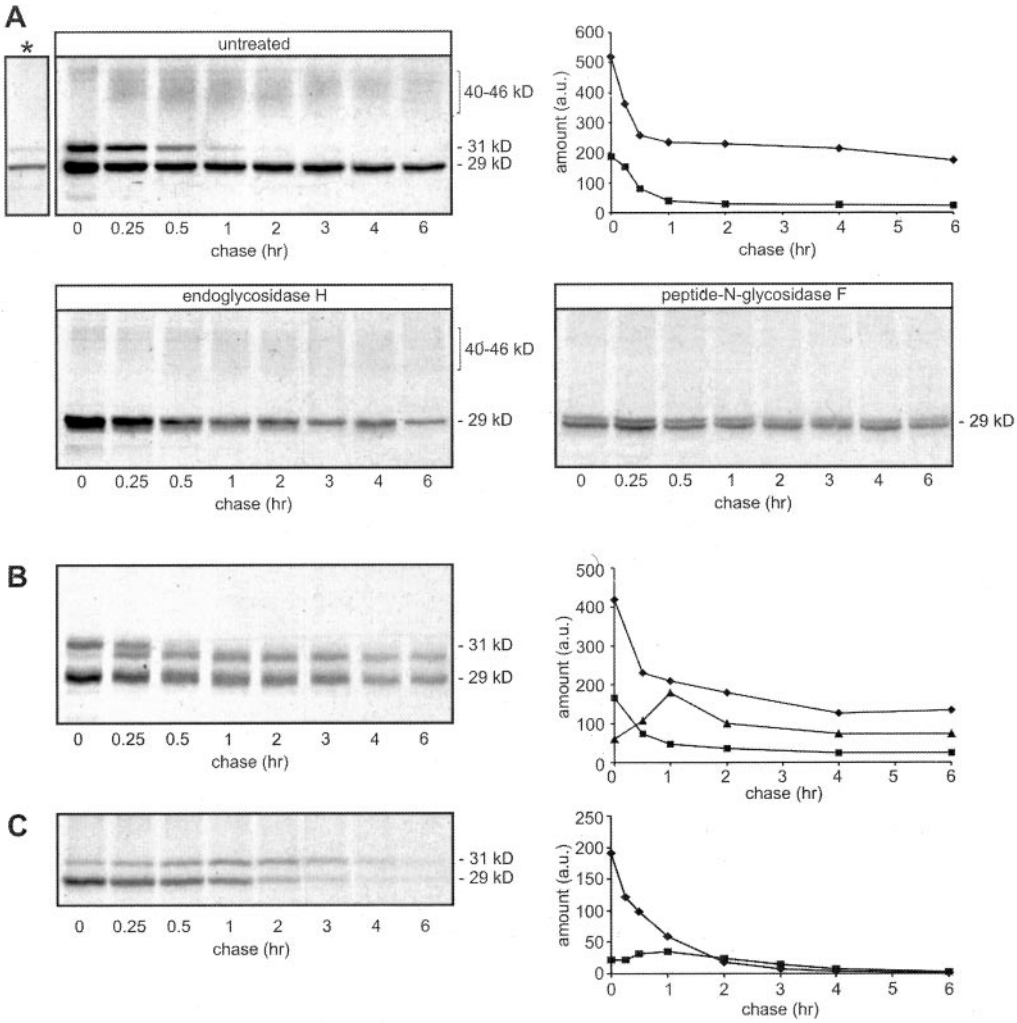

FIG. 1. **Biosynthetic maturation of AQP2.** *A*, MDCK-AQP2 cells were labeled and chased as described under "Experimental Procedures." AQP2 was immunoprecipitated, resolved by SDS-PAGE, and analyzed by phosphorimaging. Alternatively, immune complexes were eluted and digested with Endo H and PNGase F. * indicates the bands that were immunoprecipitated after a 2.5-min pulse. The 29-kDa (*diamonds*) and 31-kDa bands were quantitated by phosphorimaging. *B*, pulse-chase in CHO-15B-AQP2 cells documents a precursor-product relation between nonglycosylated (*diamonds*), high mannose form (*squares*), and mature glycosylated (*triangles*) AQP2. *C*, pulse-chase in MDCK-AQP2-R187C cells shows that the mutant in contrast to AQP2 is glycosylated progressively during the 1st h of chase (*diamonds*, nonglycosylated; *squares*, high mannose form). Data are representative of four independent experiments.

AQP2. Likely the AQP2 molecules that were synthesized at the beginning of the pulse may have already left the ER. Indeed, when the pulse is reduced to 2.5 min, we did not observe the 40–46 kDa smear (Fig. 1*A*, *lane* indicated with *). The 29-kDa form of AQP2 is a very stable molecular species. After an initial decrease during the 1st h of the chase (likely because of degradation in the ER and transport to the Golgi complex), the half-life of this form is in the order of 6–12 h. The results of the pulse-chase experiments extend and confirm earlier steady-state measurements that document that the 29-kDa band represents nonglycosylated AQP2, whereas the 31- and 40–46-kDa bands are the high mannose and the complex glycosylated forms, respectively.

Because the complex glycosylated forms of newly synthesized AQP2 ran as a faint smear between 40 and 46 kDa and because of a background signal along the entire length of the lane, an accurate quantification of the glycoforms was problematic and precluded the investigation of product precursor relationships between the various forms. To avoid this problem we expressed AQP2 in CHO-15B cells that lack functional GlcNAc transferase I (31) and do not express endogenous AQP2. This enzyme adds *N*-acetylglucosamine to mannose residues after trimming of the GlcNac2Man9Glc3 oligosaccharide by ER and Golgi mannosidases. In the absence of a functional enzyme, complex glycosylated proteins are not formed, and the resulting mannose-trimmed glycoproteins have a slightly higher mobility than the high mannose precursor. Results of pulse-chase experiments in CHO-15B-AQP2 cells are shown in Fig. 1*B*. As in MDCK cells, ~75% of newly synthesized AQP2 was present in the 29-kDa band and was not glycosylated at the end of the pulse, whereas the remainder of radioactivity was present in the 31-kDa band. During the chase period this Endo H-sensitive band (not shown) was converted to a discrete band of 30 kDa. Quantification of the three bands (Fig. 1*B*) shows a clear precursor-product link between the high mannose and the 30-kDa glycosylated forms of AQP2. The kinetics of AQP2 glycosylation in MDCK and CHO-15B cells was similar, suggesting that the limited extent of glycosylation is not a property of the cells but instead is determined by intrinsic features contained within the AQP2 molecule. As in MDCK cells, the nonglycosylated and terminally glycosylated form of wild-type AQP2 are stable proteins, whose levels decrease with a half-life of 6–12 h after the 1st h of chase, indicating that glycosylation is not essential for the stability of the wild-type protein.

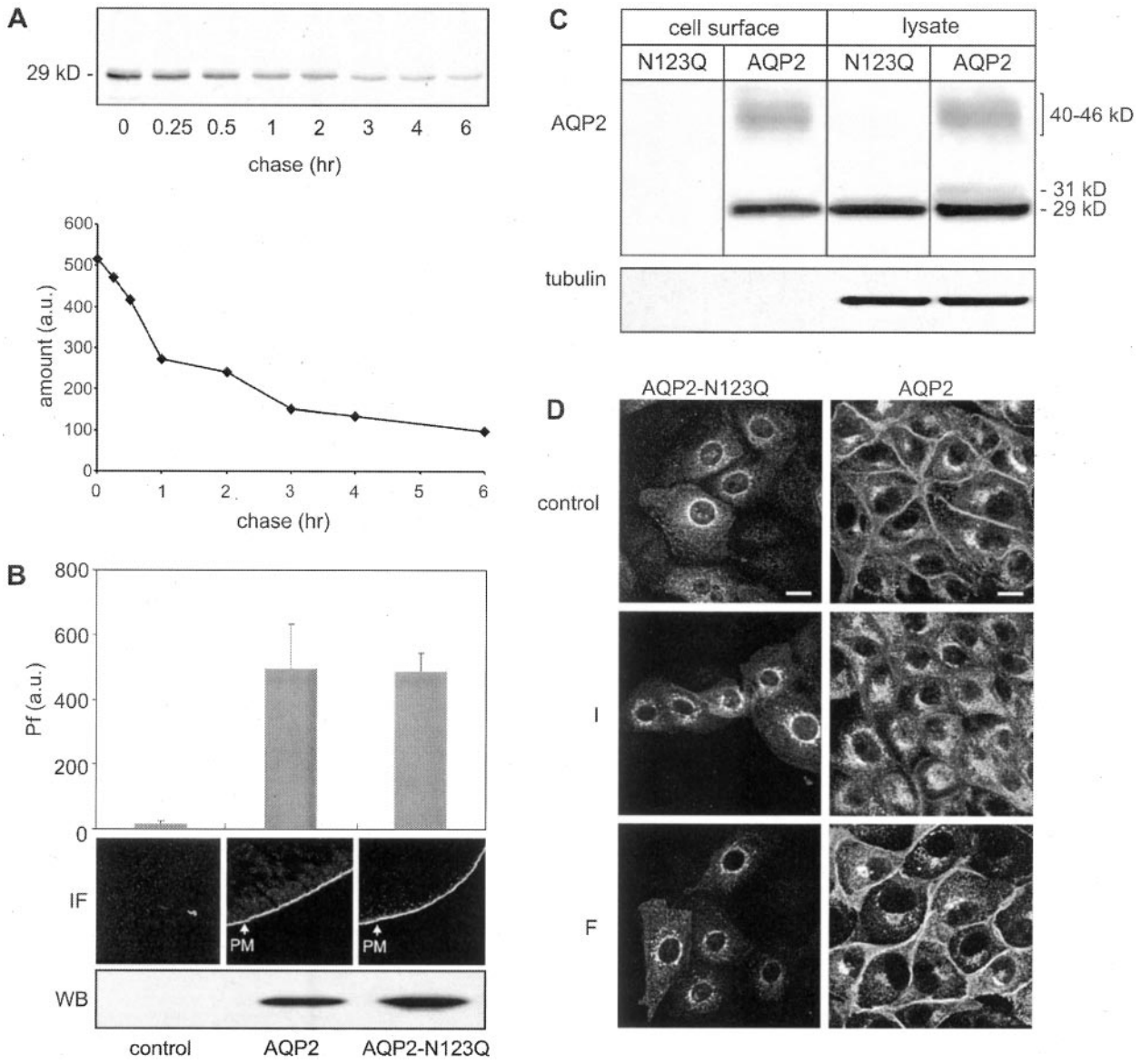

FIG. 2. **Glycosylation is essential for cell surface expression of AQP2-N123Q.** *A*, in pulse-chase and immunoprecipitation in MDCK-AQP2-N123Q cells, only a 29-kDa nonglycosylated protein could be detected. Data are representative of four independent experiments. Quantitation of the 29-kDa band was done by phosphorimaging. *B*, injection of AQP2-N123Q cRNA in *Xenopus* oocytes. Western blot (*WB*) of total membranes shows that the mutant and AQP2 are expressed at the same level. The mutant, like AQP2, localized at the plasma membrane (*IF*), whereas water permeability (*Pf*) was the same for the two proteins at 48 h postinjection. Data are the means ± S.D. of three experiments. *C*, MDCK-AQP2-N123Q and MDCK-AQP2 cells were labeled with NHS-SS-biotin on ice. Detergent lysates were split into two aliquots to determine total (20%) and cell surface AQP2. Biotinylated proteins were retrieved on neutravidin-agarose and analyzed by Western blots with antibodies against AQP2 and tubulin. Data are representative of four independent experiments. *D*, MDCK-AQP2-N123Q and MDCK-AQP2 cells were grown on coverslips and treated with 10^{-5} M indomethacin (*I*) for 16 h followed by a 1-h incubation with 10^{-5} M forskolin (*F*). AQP2 was labeled with a rabbit antibody and stained with Alexa488 goat and rabbit IgG. AQP2-N123Q is localized predominantly to a juxtanuclear structure but not to the plasma membrane. The distribution of N123Q-AQP2 is invariant to reagents that effect localization of AQP2. *Scale bar* is 20 μm.

The consensus site for *N*-linked glycosylation is located in the second extracellular loop, 7 amino acid residues upstream of the predicted fourth transmembrane domain. Efficient glycosylation requires a distance of at least 10 amino acids from a C-terminal transmembrane domain, possibly because space constraints combined with egress through the translocon limit a productive interaction with oligosaccharyltransferase (32). We therefore hypothesized that a prolonged residence time of AQP2 in the ER would increase glycosylation. To address this issue, we performed pulse-chase experiments in MDCK cells expressing vesicular stomatitis virus G-tagged AQP2-R187C (Fig. 1*C*), a mutant that is retained in the ER in recessive NDI (33). As shown in Fig. 1*C*, the amount of the high mannose precursor of the mutant continued to increase during the first 2 h of chase. This is in sharp contrast to wild-type AQP2 for which the level of the high mannose form decreased continually after the pulse (Fig. 1*A*). Thus this result suggests that prolonged residence of AQP2 in the ER enhanced the efficiency of glycosylation in a post-translational manner.

Glycosylation Is Required for Cell Surface Expression of AQP2—To analyze the function of *N*-linked glycosylation we substituted Asn^{123} for Gln and expressed this AQP2 mutant in MDCK cells. We first investigated the synthesis and stability of AQP2-N123Q in pulse-chase experiments of ^{35}S-labeled cells followed by immunoprecipitation and SDS-PAGE. As expected and shown in Fig. 2*A*, removal of the *N*-linked glycosylation consensus site did not affect expression of the nonglycosylated 29-kDa precursor; however, neither the 31-kDa nor the mature 42–46-kDa were present. Quantitation of the 29-kDa band showed that its half-time was reduced from 6–12 h in MDCK-

AQP2 cells to 4 h in the MDCK-AQP2-N123Q cells. Many glycoproteins are *O*-glycosylated in the Golgi complex. It is not known, however, whether AQPs are *O*-glycosylated. Removal of the *N*-linked glycosylation motif in AQP2 produced a protein that ran as single sharp band on SDS-polyacrylamide gels during the pulse and all chase times, suggesting that AQP2 is not *O*-glycosylated in these cells.

Given the reduced stability of the glycosylation mutant, we next addressed whether or not this protein was misfolded, using water permeability in *Xenopus* oocytes as read-out system. Although oocytes lack the mechanisms for vasopressin-regulated translocation of AQP2, they nevertheless are very valuable for determining the biophysical properties of water channels (28). We injected wild-type AQP2 and AQP2-N123Q cRNAs in *Xenopus* oocytes and measured water permeability of the plasma membrane. As documented in Fig. 2*B*, both proteins were expressed at the same level at the plasma membrane and yielded similar water permeability. This showed that the absence of glycosylation did not affect the ability of AQP2 to form functional water channels and suggests that AQP2-N123Q is not misfolded.

To investigate whether AQP2-N123Q reached the cell surface in a more physiological model, we performed cell surface biotinylation in the MDCK-AQP2-N123Q cells. Biotinylated proteins were then retrieved from detergent lysates by neutravidin-agarose precipitation, resolved by SDS-PAGE, and analyzed by Western blot. Although wild-type AQP2 was expressed at the plasma membrane, AQP2-N123Q was not detected on the cell surface (Fig. 2*C*). To rule out that the AQP2 signal on the plasma membrane was the result of cell leakage, causing biotinylation of intracellular proteins, we also analyzed the blots with a tubulin antibody. As expected, we did detect tubulin in total cell lysates; however, it was not retrieved on the neutravidin beads, showing that the plasma membrane remained intact during the experiment. Because plasma membrane expression of AQP2 can be induced by vasopressin or forskolin treatment, we added 10 μM forskolin to the cells. Even under this condition AQP2-N123Q was retained intracellularly.

The observation that AQP2-N123Q is not delivered to the cell surface suggested that the mutant either cannot leave the ER or is allowed to exit the ER but retained in another compartment. To discriminate between these possibilities, we investigated the localization of AQP2-N123Q. Cells were treated with either indomethacin or forskolin, which diminishes or enhances cAMP-dependent AQP2 expression on the apical cell surface (24), respectively. As shown in Fig. 2*D*, AQP2-N123Q is predominantly localized in perinuclear structures but not on the plasma membrane. We confirmed with confocal immunofluorescence microscopy on filter-grown AQP2-N123Q MDCK cells, that the mutant was localized intracellularly (not shown). Even though the various kinase consensus sequences are retained in the mutant, it is clear that AQP2-N123Q localization is not affected by the drugs. In contrast wild-type AQP2 is translocated to the cell surface in the presence of forskolin, whereas the level of wild-type AQP2 at the cell surface is decreased by indomethacin as was reported before (Fig. 2*D*). Thus, glycosylation of AQP2 is required for cell surface expression, and the absence of glycosylation induces intracellular retention.

Glycosylation of AQP2 Is Not Essential for Exit from the ER—To define the location where nonglycosylated AQP2 is retained, we performed double label immunofluorescence microscopy on MDCK-AQP2 and MDCK-AQP2-N123Q cells using antibodies against markers of the ER (PDI), Golgi complex (CTR433), *trans*-Golgi network (TGN) (γ-adaptin), and the cell surface (gp114). As shown in Fig. 3, AQP2-N123Q (*green*) is

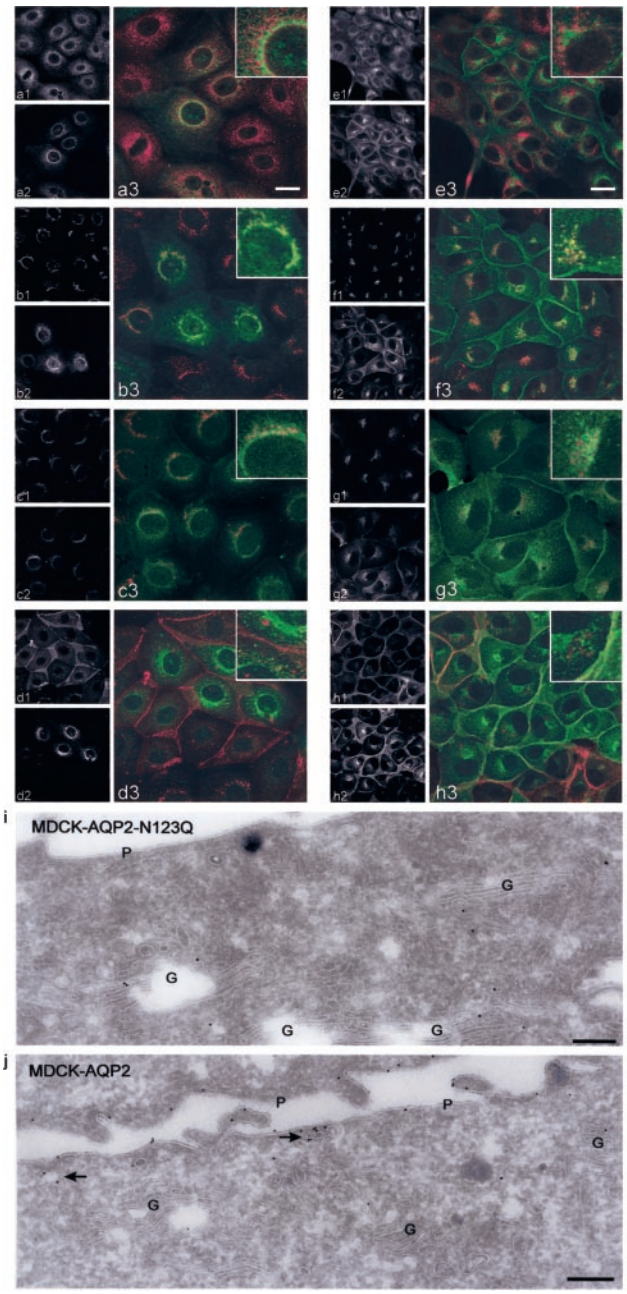

FIG. 3. **Localization of AQP2-N123Q in MDCK cells.** MDCK-AQP2-N123Q (*a1–d3*) and MDCK-AQP2 (*e1–h3*) cells were grown on coverslips and double labeled with affinity-purified guinea pig antibody against AQP2 (*a2* and *e2*) (artificial *green*) and a rabbit antibody against PDI (*a1* and *e1*) (artificial *red*), with rabbit antibody against AQP2 (*b2*, *c2*, *d2*, *f2*, *g2*, and *h2*) (*green*) and mouse antibodies against CTR433 (*b1* and *f1*) (*red*), γ-adaptin (*c1* and *g1*) (*red*), and gp114 (*d1* and *h1*) (*red*). Cells were stained with Cy3 goat anti-guinea pig IgG, Cy3 goat anti-rabbit IgG, or Alexa488 goat anti-mouse IgG. Merged images are shown, where colocalization in the same optical sections appears as *yellow* (*a3*, *b3*, *c3*, *d3*, *e3*, *f3*, *g3*, and *h3*). Note the lack of colabeling of AQP2-N123Q with PDI and gp114 and partial colocalization with CTR433 and γ-adaptin. *Scale bar* is 20 μm. Ultrathin cryosections of MDCK-AQP2-N123Q (*I*) and MDCK-AQP2 (*J*) cells were immunogold labeled for AQP2 (10-nm gold particles). Wild-type AQP2 is readily detected at the plasma membrane (*P*) and putative intracellular storage vesicles (*arrows*), whereas no or low labeling is found in the Golgi complex (*G*). In AQP2-N123Q cells the plasma membrane is not labeled, whereas staining of the Golgi complex is increased. *Scale bar* is 200 nm.

mainly in crescent structures around the nucleus and in cytoplasmic punctae in close vicinity of the perinuclear labeling. The AQP2-N123Q-containing structures are partially colabeled

with CTR433 (Fig. 3, *b3*) and γ-adaptin (Fig. 3, *c3*), but do not label for PDI (Fig. 3, *a*3), gp114 (Fig. 3, *d3*), and LAMP-2 (not shown), suggesting that the glycosylation mutant is associated predominantly with a Golgi-related organelle. The localization of the mutant with respect to the markers was independent of the confluence of the cells (not shown). In this respect AQP2-N123Q behaves similarly to the wild-type protein that also colabeled with CTR433 (Fig. 3, *f3*) and γ-adaptin (Fig. 3, *g3*), although it is clear that wild-type AQP2 is also present on the cell surface as evidenced by the overlapping distribution with gp114 (Fig. 3, *h3*). The mutant, however, was not transported to the cell surface given the lack of colabeling with gp114.

Because light microscopy suggested that the glycosylation mutant escaped the ER and localized to Golgi related structures, we next used immunogold electronmicroscopy on ultrathin cryosections to confirm this observation. As shown in Fig. 3*J*, wild-type AQP2 was found predominantly at the plasma membrane and in tubulovesicular structures in the apical cytoplasm, whereas little if any gold particles were present in the ER (not shown) and Golgi complex as we reported before in *Xenopus* oocytes (27). In contrast to wild-type AQP2 and in agreement with the biochemical data, AQP2-N123Q (Fig. 3*I*) was not distributed to the apical cell surface. Interestingly, most of the gold particles localized to the Golgi apparatus and associated vesicular structures, whereas little if any AQP2-N123Q was associated with the ER (not shown). The steep reduction of the number of gold particles in post-Golgi compartments in AQP2-N123Q-expressing cells compared with the wild-type situation suggested that glycosylation of AQP2 is a sorting determinant for exit from the Golgi complex, rather than for export from the ER.

Brefeldin A-induced Redistribution of AQP2-N123Q—As a final test to assess whether or not AQP2-N123Q was transported beyond the Golgi complex, we used the fungal metabolite brefeldin A (BFA). This drug inhibits ADP-ribosylation factor exchange factors, dissociates many peripheral membrane proteins from the Golgi complex, fragments the Golgi matrix into the cytoplasm, and collapses the Golgi complex into the ER (34). If a protein is associated with the Golgi complex, a short term BFA treatment should perturb its intracellular distribution and may lead to any of the above described localization phenotypes. Proteins that are in post-Golgi compartments, however, are not retrieved under the same experimental conditions to the ER. Instead these require much longer incubation times to be relocalized to the ER (35). Because the Golgi complex in MDCK cells is resistant to BFA (36), we generated stable CHO transfectants expressing AQP2 or AQP2-N123Q to perform these experiments. As shown in Fig. 4, AQP2-N123Q was localized in an intracellular compartment and was not present on the plasma membrane, whereas wild-type AQP2 resided both on the cell surface and intracellularly as in MDCK cells. Addition of 5 μg/ml BFA for 30 min had a small effect on the localization of wild-type AQP2, which now partially codistributed with the transfected TGN membrane marker GFP-furin in a condensed perinuclear structure (Fig. 4). As positive controls for BFA activity we confirmed that it caused dissociation of γ-adaptin into the cytoplasm and a redistribution of the Golgi matrix protein GM130 into scattered cytoplasmic structures (Fig. 4) as was shown by others before (37, 38). AQP2-N123Q localization was changed dramatically by BFA from the crescent shaped structure(s) in the control cells to a condensed spot in the perinuclear region which also contained GFP-furin (Fig. 4). Identical results were obtained when incubations were extended to 1 h with 10 μg/ml BFA (not shown). It is of interest to note that the double label experiments in control cells with the markers of different Golgi subcompartments reveal better

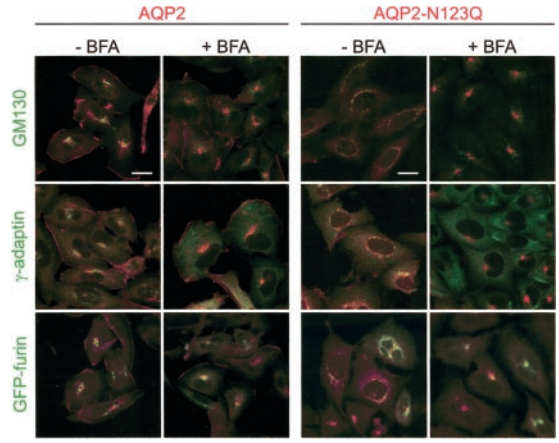

FIG. 4. **Distribution of AQP2-N123Q is sensitive to BFA.** CHO-AQP2-N123Q and CHO-AQP2 transfectants were or were not transfected with furin-pEGFP and grown on coverslips to subconfluence. Cells were incubated for 30 min with or without 5 μg/ml BFA and fixed with 3% paraformaldehyde. AQP2 (*red*) was labeled with a rabbit antibody and stained with Alexa568 goat anti-rabbit IgG. GM130 (*green*) and γ-adaptin (*green*) were labeled with mouse antibodies and stained with Alexa488 goat anti-mouse IgG. BFA caused dissociation of γ-adaptin from the TGN and vesiculation of the Golgi complex as shown by the distribution of GM130. Note that BFA has little effect on the distribution of wild-type AQP2, whereas the localization of AQP2-N123Q changed from the crescent structure around the nucleus to a concentrated spot and scattered structures in the perinuclear cytoplasm. *Scale bar* is 20 μm.

colabeling with AQP2-N123Q than with wild-type AQP2. This would be consistent with previous observations that a large pool of intracellular wild-type AQP2 is in storage vesicles representing a post-Golgi compartment. Collectively, the biochemical and morphological data show that glycosylation of AQP2 is not essential for export from the ER but is a critical determinant for exit from the Golgi complex.

Tetramerization of AQP2 Occurs in the ER and Does Not Require Glycosylation—The AQP2 homotetramer forms a functional water pore in the apical plasma membrane. Oligomerization of transport channels has been reported to occur both in the ER (39) and in the TGN (40). So far it has not been established where tetramerization of AQP2 occurs and whether glycosylation is a prerequisite for tetramerization. To address these issues we pulse labeled MDCK-AQP2 cells for 30 min with [^{35}S]methionine/cysteine. At this time point a significant fraction of the AQP2 molecules is in the high mannose form and sensitive to Endo H (Fig. 1*A*), consistent with a localization in the ER. The cells were chased for 0, 1, and 3 h, homogenized, and a solubilized total membrane fraction was resolved by velocity gradient centrifugation. AQP2 was detected by immunoprecipitation of the gradient fractions and quantitated by phosphorimaging. Previous studies validated this method to separate AQP2 monomers and tetramers (19). Already after 30 min of labeling, most of AQP2 distributed in the high density fractions of the gradient, corresponding to a position where tetrameric AQP2 sediments. At this time point, we found tailing of the tetrameric pool into the low density fractions where monomeric AQP2 sedimented (Fig. 5*A*). This probably represented AQP2 molecules that have not been incorporated in stable tetramers. Importantly, we detected the high mannose (ER) form in the high density gradient fractions showing that tetramerization occurred in the ER. After 1 and 3 h of chase, AQP2 disappeared from the low density fractions and was concentrated in fractions 1–3 containing tetrameric AQP2. The mature glycosylated form was not detectable because the signal is already weak in the direct immunoprecipitations (see Fig. 1*A*) and is diluted further over nine fractions of the gradient.

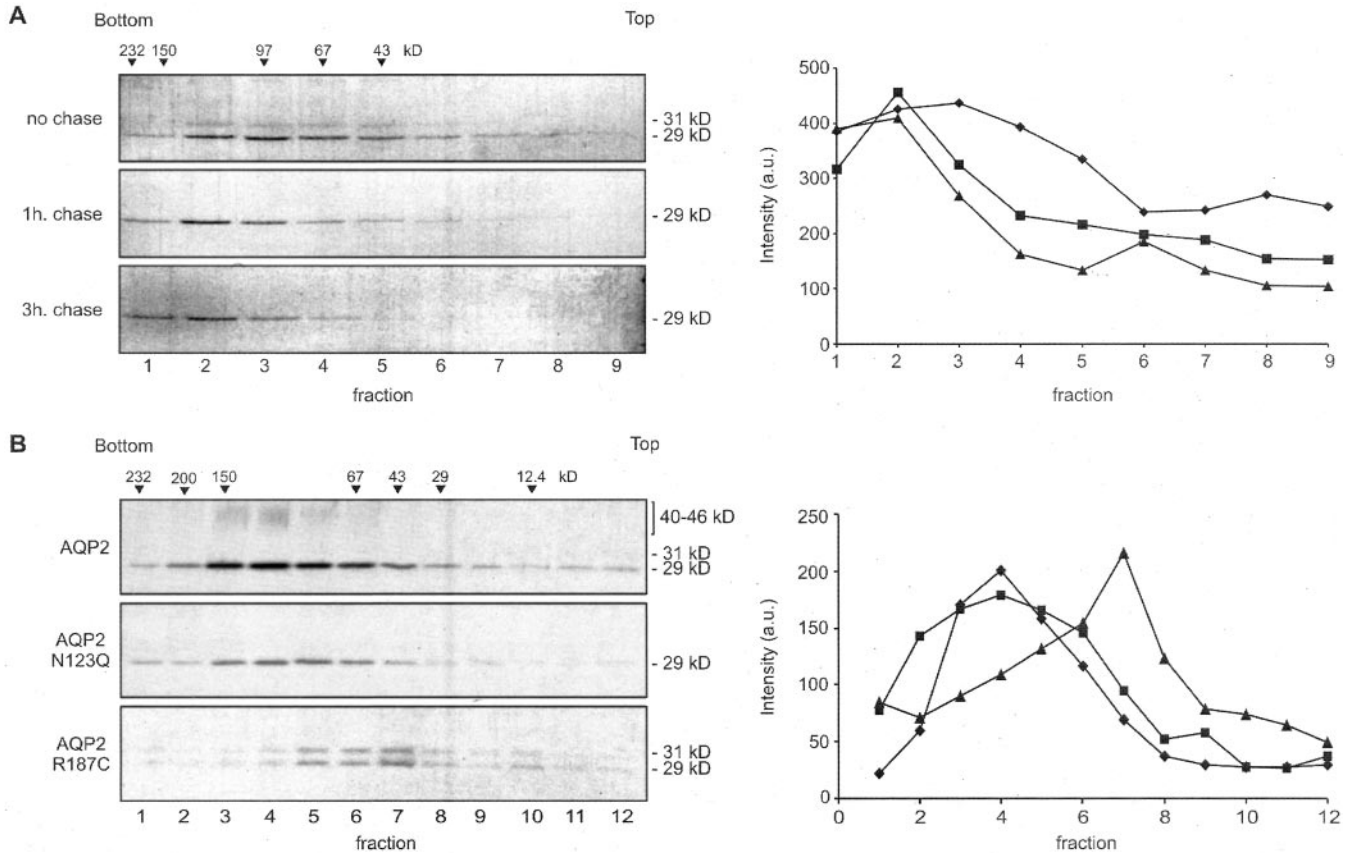

FIG. 5. **AQP2 tetramerizes independent of glycosylation in the ER.** *A*, MDCK-AQP2 cells were labeled for 30 min with [^{35}S]methionine/cysteine and chased for the indicated periods of time. Membranes were isolated and solubilized in 4% deoxycholate at the end of the chase period. Detergent lysates were layered on top of 5–17.5% sucrose gradient, containing 0.1% Triton X-100. Gradients were centrifuged at 8 °C for 18 h at 150,000 × *g*. AQP2 was immunoprecipitated from 1-ml gradient fractions and resolved on SDS-polyacrylamide gels. Parallel gradients with sedimentation markers, ovalbumin (43 kDa), bovine serum albumin (67 kDa), phosphorylase *b* (97 kDa), yeast alcohol dehydrogenase (150 kDa), and catalase (232 kDa) were run simultaneously, and *arrowheads* denote marker positions. Note that high mannose-glycosylated AQP2 could be detected at the end of the pulse (*diamonds*) in gradient fractions containing tetrameric AQP2. This band had disappeared after a 1-h chase (*squares*) and 3 h (*triangles*), consistent with maturation of AQP2 (see Fig. 1*A*). *B*, membranes were prepared from MDCK-AQP2-N123Q (*squares*), MDCK-AQP2-R187C (*triangles*), and MDCK-AQP2 (*diamonds*) cells. Solubilized membranes were loaded on 5–17.5% sucrose gradients and centrifuged as described above. Gradient fractions of 0.5 ml were analyzed by Western blot with AQP2 antibodies and quantitated by densitometry. AQP2-N123Q peak fractions were in the same region as those of wild-type AQP2, showing that AQP2-N123Q can tetramerize. As negative control we used membranes prepared from AQP2-R187C cells. This mutant does not leave the ER, fails to oligomerize, and is found in gradient fractions with a lower sucrose density. Data are representative of three independent experiments.

The availability of the glycosylation-deficient AQP2-N123Q mutant that is able to exit the ER allowed us to investigate whether or not glycosylation is a prerequisite for tetramerization. Membranes were isolated from MDCK-AQP2-N123Q transfectants and solubilized as above. Gradient fractions were then analyzed by Western blot and quantitated with Imagequant™ for the presence of AQP2-N123Q. As controls we used membranes from transfectants expressing wild-type-AQP2 and membranes isolated from MDCK cells expressing vesicular stomatitis virus G-tagged AQP2-R187C. This recessive NDI mutant is unable to form tetramers (19). Results of this experiment are shown in Fig. 5*B*, which documents that AQP2-N123Q is distributed to the same fractions as tetrameric wild-type AQP2, but not to the peak fractions where monomeric AQP2-R187C sedimented. Thus tetramerization of AQP2 occurs independently of glycosylation.

DISCUSSION

The vasopressin-regulated water channel AQP2 is an important protein for water homeostasis in humans because mutations in AQP2 result in the development of NDI (28). Nearly a decade since the discovery, it has not been established rigorously where tetramerization of AQP2 occurs and what the significance of glycosylation is for the function of this water channel. Using the MDCK model system we found that tetramerization of newly synthesized AQP2 occurs during or shortly after translocation in the ER. Ectopic expression of a glycosylation mutant in MDCK cells revealed that *N*-linked glycosylation is essential for the expression of AQP2 water channels at the cell surface. Two pieces of experimental evidence show that the absence of *N*-glycans in AQP2-N123Q does not result in severe folding defects. This mutant, like wild-type AQP2, oligomerizes in the ER and is exported from the ER in transfected MDCK cells, although the half-life of the protein is somewhat shortened to 4 h. Second, AQP2-N123Q localized to the plasma membrane in *Xenopus* oocytes and more importantly, conferred the same water permeability as wild-type AQP2. It has been found earlier that membrane proteins can be expressed on the cell surface of *Xenopus* oocytes but fail to do so when transfected in mammalian cells. Because *Xenopus* oocytes are usually maintained below 20 °C and mammalian cells at 37 °C, different localizations in the two experimental systems likely reflect the general phenomenon that reduced temperature increases cell surface expression (41).

The observation that oligomerization of wild-type AQP2 and AQP2-N123Q occurred in the ER is novel and has implications for our understanding of the formation of heterotetramers in

dominant NDI. Based on earlier observations on the assembly of connexin43 oligomers in the Golgi complex (40), we postulated that AQP2 oligomerizes after its exit from the ER (19). Because AQP2 mutants in dominant NDI acquire complex type *N*-glycans, they pass ER quality control mechanisms and are transported to the Golgi complex. At this location they might oligomerize either via a stochastic process or by selective incorporation in microdomains that would facilitate coassembly of mutant and wild-type AQP2 in heterotetramers that fail to be targeted properly to the apical plasma membrane.

The tetramerization experiments described here suggest a different scenario in which wild-type and mutant AQP2 already oligomerize in the ER and are then transported to a destination dictated by molecular features contained within the mutant water channel subunit. Alternatively, the productive assembly of AQP2 into a tetramer requires a sequential series of precisely orchestrated events in the ER. Although mutants in dominant NDI do assemble with wild-type molecules in a tetramer, the cell may nevertheless harbor surveillance systems that monitor the unusual composition of these tetramers. Possibly, the complexes of wild-type and mutant AQP2 protein might take an alternative ER export pathway to the Golgi complex as has been shown for the cystic fibrosis transmembrane conductance regulator (42). Further experiments are needed to discriminate between these possibilities because the molecular mechanisms and transport routes directing trafficking of wild-type AQP2 from the ER to the Golgi complex and endosomal compartments have not been defined.

Our pulse-chase experiments showed that only 25% of newly synthesized AQP2 is glycosylated. Using steady-state measurements in renal specimen, the same substoichiometric glycosylation was found for AQP1 (14), whereas 34% of AQP2 was glycosylated (15). The limited glycosylation of AQP2 molecules is likely caused by steric constraints that are imposed by the close proximity of the glycosylation site to the two adjacent transmembrane domains. Glycosylation mapping experiments with Na,K-ATPase-β isoforms showed that the degree of glycosylation of such sites increases with the time spent in the ER (43). Support for this idea is provided by the results of the pulse-chase experiments with AQP2-R187C. Like wild-type AQP2, 25% of this mutant is glycosylated at the end of the pulse. During the 1st h of the chase, the amount of the mutant that gets glycosylated is doubled. This suggests that the prolonged residence time of the mutant in the ER compared with that of wild-type AQP2 favors interactions with the oligosaccharyltransferase, thereby allowing for post-translational glycosylation. A survey of other AQP2 mutants that are retained in the ER shows that these all have increased *N*-linked glycosylation (17, 44, 45). The lack of glycosylation of AQP2-T125M, however, is immaterial for its role in recessive NDI. This is best appreciated from a comparison with AQP2-N123Q. Although AQP2-T125M was retained intracellularly in oocytes (17, 44, 45), we here showed that AQP2-N123Q was localized exclusively on the plasma membrane in this experimental system. The dichotomy between the two mutants indicates that the T125M mutation likely introduced less subtle structural alterations in AQP2 than the N123Q mutation, the consequence of which might be that AQP2-T125M is better recognized by quality control mechanisms as a misfolded protein than AQP2-N123N.

Earlier studies with tunicamycin reported that glycosylation is not required for vasopressin-dependent transport of AQP2 (15) in filter-grown MDCK cells. Our results complement and extend these data and may explain why the glycosylation inhibitor has little influence on AQP2-dependent water permeability. We used the N123Q mutant because recent studies document that tunicamycin has many side effects within a short period after its administration to cells. These include activation of ER transcription factors (21) and the induction of a stress response that regulates many aspects of membrane transport and lipid biogenesis (22). Because the half-life of newly synthesized AQP2 molecules is in the order of 12 h (Fig. 1), ~25% of the existing (glycosylated) AQP2 pool is still present at the end of a 24-h tunicamycin incubation. This is a conservative estimate as we found that the synthesis rate of AQP2 in confluent filter-grown MDCK cells is 20 times lower than in semiconfluent cells grown on plastic (not shown). These AQP2 molecules are already transported beyond the ER, are not sensitive to tunicamycin, and most likely reside in the post-Golgi, cAMP-sensitive subapical storage site. The main effect of vasopressin or forskolin is the activation of a cAMP signal transduction pathway which ultimately results in the phosphorylation of serine 256 in AQP2 and enhanced exocytosis of storage vesicles to the apical cell surface. Accordingly, any wild-type AQP2 molecule in the post-Golgi storage compartment, be it glycosylated or not, is a substrate for protein kinase A and would be targeted to the cell surface. In contrast, the N123Q mutant that is not transported beyond the Golgi complex never reaches this storage compartment and therefore fails to be transported to the cell surface in the presence of drug-enhanced cAMP levels.

N-Linked glycosylation is important for many cellular processes, including protein folding. When glycosylation is inhibited, the most commonly reported effect is the production of misfolded, often aggregated proteins that do not mature into a functional state (see Ref. 46). Other glycoproteins, however, do not rely for their function on added *N*-linked glycans. This suggests that oligosaccharides may have a local effect on protein folding, possibly depending on the environment of the *N*-linked glycosylation sites. Although removal of the glycosylation site in AQP2-N123Q produces a protein with a reduced half-life, it is of interest to note that the same result was found for AQP2-S256D and AQP2-E258K, two mutants in the C-terminal tail, whose glycosylation is indiscernible from wild-type AQP2 (not shown). Obviously, glycosylation *per se* is not important for AQP2 folding, suggesting that AQP2 folding is not dependent on the primary calnexin-calreticulin ER quality control mechanisms (46). Additional post-ER quality control mechanisms have been described for the recognition and sorting of misfolded proteins to degradative compartments. In yeast, the Tul1 transmembrane ubiquitin ligase has been identified which ubiquitinates and sorts membrane proteins with polar transmembrane domains to multivesicular bodies for degradation (47). Although charged residues are not frequently encountered in single transmembrane domains, they are quite common in polytopic membrane proteins, including AQP2. Because AQP2 is not known to be ubiquitinated, the significance of post-ER quality control, however, awaits further experimentation.

Instead we found that the intracellular itinerary of this water channel in MDCK cells is critically dependent on the presence of *N*-linked glycans. In the absence of *N*-glycans, AQP2 travels to the Golgi complex but does not reach the apical plasma membrane. *N*-Linked glycosylation and lipid rafts are thought to be involved in apical targeting as was shown earlier for artificial model proteins (48, 49). Because we and others (50) found that AQP2 is soluble in Triton X-100 at 4 °C (not shown), lipid rafts do not seem to play a critical role in apical transport of AQP2. It is more likely that the *N*-glycan of AQP2 serves an essential function in its sorting in the Golgi complex. Indeed, binding of cargo glycoproteins to the L-type lectins VIP36 and ERGIC-53, which are predominantly localized in post-ER compartments, has been proposed to be important for

their sorting (see Ref. 51). Interestingly the function of ER-GIC-53 appears to be controlled by VIPL, another L-type lectin localized to the ER (52). Alternatively, or in addition, export of AQP2 from the TGN and its packaging into apical transport vesicles might require interactions of its *N*-glycan with a putative lectin (see Ref. 53).

Finally, although AQP2-N123Q passed ER quality control mechanisms, there might be subtle differences between the mutant and nonglycosylated wild-type AQP2 that could contribute to the transport phenotype of the mutant that we observed in our experiments. Irrespective of the precise mechanisms, it is clear that glycosylation of AQP2 is important for its ability to function as a water channel on the cell surface. The nonglycosylated subunits may be targeted via a piggy-back mechanism with the glycosylated subunit to the plasma membrane. Experiments are currently under way to test this hypothesis.

Acknowledgments—We are grateful to Ger Strous and Bertrand Kleizen for reading the manuscript and Ineke Braakman for many helpful suggestions. We thank Michel Bornens, Ineke Braakman, Kai Simons, and Gary Thomas for generously providing reagents.

REFERENCES

1. Kozono, D., Yasui, M., King, L. S., and Agre, P. (2002) *J. Clin. Invest.* **109,** 1395–1399
2. Murata, K., Mitsuoka, K., Hirai, T., Walz, T., Agre, P., Heymann, J. B., Engel, A., and Fujiyoshi, Y. (2000) *Nature* **407,** 599–605
3. Nielsen, S., Frokjaer, J., Marples, D., Kwon, T. H., Agre, P., and Knepper, M. A. (2002) *Physiol. Rev.* **82,** 205–244
4. Klussmann, E., Tamma, G., Lorenz, D., Wiesner, B., Maric, K., Hofmann, F., Aktories, K., Valenti, G., and Rosenthal, W. (2001) *J. Biol. Chem.* **276,** 20451–20457
5. Fushimi, K., Sasaki, S., and Marumo, F. (1997) *J. Biol. Chem.* **272,** 14800–14804
6. van Balkom, B. W. M., Savelkoul, P. J. M., Markovich, D., Hofman, E., Nielsen, S., van der Sluijs, P., and Deen, P. M. T. (2002) *J. Biol. Chem.* **277,** 41473–41479
7. Kamsteeg, E. J., Heijnen, I., van Os, C. H., and Deen, P. M. T. (2000) *J. Cell Biol.* **151,** 919–929
8. Bryant, N. J., Govers, R., and James, D. E. (2002) *Nat. Rev. Mol. Cell Biol.* **3,** 267–277
9. Gouraud, S., Laera, A., Calmita, G., Carmosini, M., Procino, G., Rosetto, O., Mannucci, R., Rosenthal, W., Svelto, M., and Valenti, G. (2002) *J. Cell Sci.* **115,** 3667–3674
10. Skach, W. R., Shi, L., Calayag, M. C., Frigeri, A., Lingapppa, V. R., and Verkman, A. S. (1994) *J. Cell Biol.* **125,** 803–815
11. Dohke, Y., and Turner, R. J. (2002) *J. Biol. Chem.* **277,** 15215–15219
12. Madrid, R., Le Maout, S., Barrault, M. B., Janvier, K., Benichou, S., and Merot, J. (2001) *EMBO J.* **20,** 7008–7021
13. Yasui, M., Hazama, A., Kwon, T. H., Nielsen, S., Guggino, W. B., and Agre, P. (1999) *Nature* **402,** 184–187
14. Smith, B. L., Preston, G. M., Spring, F. A., Anstee, D. J., and Agre, P. (1994) *J. Clin. Invest.* **94,** 1043–1049
15. Baumgarten, R., van de Pol, M. H. J., Wetzels, J. F. M., van Os, C. H., and Deen, P. M. T. (1998) *J. Am. Soc. Nephrol.* **9,** 1553–1559
16. Goji, K., Kuwahara, M., Gu, Y., Matsuo, M., Marumo, F., and Sasaki, S. (1998) *J. Clin. Endocrinol. Metab.* **83,** 3205–3209
17. Marr, N., Bichet, D. G., Hoefs, S., Savelkoul, P. J. M., Konings, I. B. M., de Mattia, F., Graat, M. P. J., Arthus, M. F., Lonergan, M., Fujiwara, T. M., Knoers, N. V. A. M., Landau, D., Balfe, W. J., Oksche, A., Rosenthal, W., Müller, D., van Os, C. H., and Deen, P. M. T. (2002) *J. Am. Soc. Nephrol.* **13,** 2267–2277
18. Morello, J. P., and Bichet, D. G. (2001) *Annu. Rev. Physiol.* **63,** 607–630
19. Kamsteeg, E. J., Wormhoudt, T. A. M., Rijss, J. P. L., van Os, C. H., and Deen, P. M. T. (1999) *EMBO J.* **18,** 2394–2400
20. Marr, N., Bichet, D. G., Lonergan, M., Arthus, M. F., Jeck, N., Seyberth, H. W., Rosenthal, W., van Os, C. H., Oksche, A., and Deen, P. M. T. (2002) *Hum. Mol. Genet.* **11,** 779–789
21. Ye, J., Rawson, R. B., Komuro, R., Chen, X., Dave, U. P., Prywes, R., Brown, M. S., and Goldstein, J. L. (2000) *Mol. Cell* **6,** 1355–1364
22. Travers, K. J., Patil, C. K., Wodicka, L., Lockhart, D. J., Weissman, J. S., and Walter, P. (2000) *Cell* **101,** 249–258
23. Deen, P. M. T., van Aubel, R. A., van Lieburg, A. F., and van Os, C. H. (1996) *J. Am. Soc. Nephrol.* **7,** 836–841
24. Deen, P. M. T., Rijss, J. P. L., Mulders, S. M., Errington, R. J., van Baal, J., and van Os, C. H. (1997) *J. Am. Soc. Nephrol.* **8,** 1493–1501
25. Braakman, I., Litty, H. H., Wagner, K. R., and Helenius, A. (1991) *J. Cell Biol.* **114,** 401–411
26. Liou, W., Geuze, H. J., Geelen, M. J. H., and Slot, J. W. (1997) *J. Cell Biol.* **136,** 61–70
27. Mulders, S. M., Bichet, D. G., Rijss, J. P. L., Kamsteeg, E. J., Arthus, M. F., Lonergan, M., Fujiwara, M., Morgan, K., Leijendekker, R., van der Sluijs, P., van Os, C. H., and Deen, P. M. T. (1998) *J. Clin. Invest.* **102,** 57–66
28. Deen, P. M. T., Verdijk, M. A., Knoers, N. V. A. M., Wieringa, B., Monnens, L. A. H., van Os, C. H., and van Oost, B. A. (1994) *Science* **264,** 92–95
29. Deneka, M., Neeft, M., Popa, I., van Oort, M., Sprong, H., Oorschot, V., Klumperman, J., Schu, P., and van der Sluijs, P. (2003) *EMBO J.* **22,** 2645–2657
30. Horwitz, M. S., Scharff, M. D., and Maizel, J. V. J. (1969) *Virology* **39,** 682–694
31. Schlesinger, S., Gottlieb, C., Feil, P., Gelb, N., and Kornfeld, S. (1975) *J. Virol.* **17,** 239–246
32. Nilsson, I., and von Heijne, G. (2000) *J. Biol. Chem.* **275,** 17338–17343
33. Deen, P. M. T., Croes, H., van Aubel, R. A., Ginsel, L. A., and van Os, C. H. (1995) *J. Clin. Invest.* **95,** 2291–2296
34. Lippincott-Schwartz, J., Yuan, L. C., Bonifacino, J. S., and Klausner, R. D. (1989) *Cell* **58,** 801–813
35. Miesenböck, G., and Rothman, J. E. (1995) *J. Cell Biol.* **129,** 309–320
36. Hunziker, W., Whitney, J. A., and Mellman, I. (1991) *Cell* **67,** 617–627
37. Robinson, M. S., and Kreis, T. E. (1992) *Cell* **69,** 129–138
38. Seemann, J., Jokitalo, E., Pypaert, M., and Warren, G. (2000) *Nature* **407,** 1022–1026
39. Geering, K., Begah, A., Good, P., Girardet, S., Roy, S., Schaer, D., and Jaunin, P. (1996) *J. Cell Biol.* **133,** 1193–1204
40. Musil, L., and Goodenough, D. A. (1993) *Cell* **74,** 1053–1063
41. Ljunggren, H. G., Stam, N. J., Ohlen, C., Neefjes, J. J., Höglund, P., Heemels, M. T., Bastin, J., Schumacher, T. N. M., Townsend, A., Kärre, K., and Ploegh, H. L. (1990) *Nature* **346,** 476–480
42. Yoo, J.-S., Moyer, B. D., Bannykh, S., Yoo, H.-M., Riordan, J. R., and Balch, W. E. (2002) *J. Biol. Chem.* **277,** 11401–11409
43. Hasler, U., Greasly, P. J., von Heijne, G., and Geering, K. (2000) *J. Biol. Chem.* **275,** 29011–29022
44. Mulders, S. M., Knoers, N. V. A. M., van Lieburg, A. F., Monnens, L. A. H., Leumann, E., Schober, E., Rijss, J. P. L., van Os, C. H., and Deen, P. M. T. (1997) *J. Am. Soc. Nephrol.* **8,** 242–248
45. Tamarappoo, B. K., and Verkman, A. S. (1998) *J. Clin. Invest.* **101,** 2257–2267
46. Ellgaard, L., and Helenius, A. (2003) *Nat. Rev. Mol. Cell Biol.* **4,** 181–191
47. Reggiori, F., and Pelham, H. R. B. (2002) *Nat. Cell Biol.* **4,** 117–123
48. Scheiffele, P., Peranen, J., and Simons, K. (1995) *Nature* **378,** 96–98
49. Gut, A., Kappeler, F., Hyka, N., Balda, M. S., Hauri, H. P., and Matter, K. (1998) *EMBO J.* **17,** 1919–1929
50. Tamarappoo, B. K., Yang, B., and Verkman, A. S. (1999) *J. Biol. Chem.* **274,** 34825–34831
51. Schrag, J. D., Procopio, D. O., Cygler, M., Thomas, D. Y., and Bergeron, J. J. M. (2003) *Trends Biochem. Sci.* **28,** 49–57
52. Nufer, O., Mitorvic, S., and Hauri, H. P. (2003) *J. Biol. Chem.* **278,** 15886–15896
53. Fiedler, K., and Simons, K. (1995) *Cell* **81,** 309–311

Glycosylation Is Important for Cell Surface Expression of the Water Channel Aquaporin-2 but Is Not Essential for Tetramerization in the Endoplasmic Reticulum

Giel Hendriks, Marco Koudijs, Bas W. M. van Balkom, Viola Oorschot, Judith Klumperman, Peter M. T. Deen and Peter van der Sluijs

J. Biol. Chem. 2004, 279:2975-2983.
doi: 10.1074/jbc.M310767200 originally published online October 30, 2003
